NAVAL POSTGRADUATE SCHOOL

MONTEREY, CALIFORNIA

THESIS

COUPLED DIRECTIONAL STABILITY OF MULTIPLE SHIP FORMATIONS

by

Ufuk Babaoglu

June 2013

Thesis Advisor: Fotis A. Papoulias
Co-Advisor: Oleg Yakimenko

THIS PAGE INTENTIONALLY LEFT BLANK

REPORT DOCUMENTATION PAGE			*Form Approved OMB No. 0704-0188*
Public reporting burden for this collection of information is estimated to average 1 hour per response, including the time for reviewing instruction, searching existing data sources, gathering and maintaining the data needed, and completing and reviewing the collection of information. Send comments regarding this burden estimate or any other aspect of this collection of information, including suggestions for reducing this burden, to Washington headquarters Services, Directorate for Information Operations and Reports, 1215 Jefferson Davis Highway, Suite 1204, Arlington, VA 22202-4302, and to the Office of Management and Budget, Paperwork Reduction Project (0704-0188) Washington DC 20503.			
1. AGENCY USE ONLY ***(Leave blank)***	**2. REPORT DATE** June 2013	**3. REPORT TYPE AND DATES COVERED** Master's Thesis	
4. TITLE AND SUBTITLE COUPLED DIRECTIONAL STABILITY OF MULTIPLE SHIP FORMATIONS		**5. FUNDING NUMBERS**	
6. AUTHOR(S) Ufuk Babaoglu			
7. PERFORMING ORGANIZATION NAME(S) AND ADDRESS(ES) Naval Postgraduate School Monterey, CA 93943-5000		**8. PERFORMING ORGANIZATION REPORT NUMBER**	
9. SPONSORING /MONITORING AGENCY NAME(S) AND ADDRESS(ES) N/A		**10. SPONSORING/MONITORING AGENCY REPORT NUMBER**	
11. SUPPLEMENTARY NOTES The views expressed in this thesis are those of the author and do not reflect the official policy or position of the Department of Defense or the U.S. Government. IRB Protocol number ____N/A____.			
12a. DISTRIBUTION / AVAILABILITY STATEMENT Approved for public release; distribution is unlimited		**12b. DISTRIBUTION CODE**	

13. ABSTRACT (maximum 200 words)

This thesis addresses the problem of coordinated motion control and the stability loss of surface marine vehicles. The mathematical model is based on Nomoto's second order model which captures the fundamental dynamics of turning on the horizontal plane with no side slip. A state feedback control law is coupled with a line of sight guidance law to provide path control. A string of three vehicles is considered where each vehicle is using the vehicle in the front as a reference point. The coupled motion stability of the formation is analyzed by linearization. It is shown that under the assumed dynamics, guidance, and control laws, the stability properties of the system decoupled into individual vehicles. This makes it possible to obtain exact analytical results that can be used in design. Parametric runs and sensitivity analysis studies show the effect of main vehicle geometric parameters on formation control and motion stability.

14. SUBJECT TERMS String stability, Platoon, Surface marine vessel, Path control, Control law, Guidance law, Eigenvalues, Damping ratio, Natural frequency			**15. NUMBER OF PAGES** 71
			16. PRICE CODE
17. SECURITY CLASSIFICATION OF REPORT Unclassified	**18. SECURITY CLASSIFICATION OF THIS PAGE** Unclassified	**19. SECURITY CLASSIFICATION OF ABSTRACT** Unclassified	**20. LIMITATION OF ABSTRACT** UU

NSN 7540-01-280-5500 Standard Form 298 (Rev. 2-89)
Prescribed by ANSI Std. 239-18

THIS PAGE INTENTIONALLY LEFT BLANK

Approved for public release; distribution is unlimited

COUPLED DIRECTIONAL STABILITY OF MULTIPLE SHIP FORMATIONS

Ufuk Babaoglu
Lieutenant Junior Grade, Turkish Navy
B.S., Turkish Naval Academy, 2007

Submitted in partial fulfillment of the
requirements for the degree of

MASTER OF SCIENCE IN MECHANICAL ENGINEERING

from the

NAVAL POSTGRADUATE SCHOOL
June 2013

Author: Ufuk Babaoglu

Approved by: Fotis A. Papoulias
Thesis Advisor

Oleg Yakimenko
Thesis Co-Advisor

Knox T. Millsaps
Chair, Department of Mechanical and Aerospace Engineering

THIS PAGE INTENTIONALLY LEFT BLANK

ABSTRACT

This thesis addresses the problem of coordinated motion control and the stability loss of surface marine vehicles. The mathematical model is based on Nomoto's second order model which captures the fundamental dynamics of turning on the horizontal plane with no side slip. A state feedback control law is coupled with a line of sight guidance law to provide path control. A string of three vehicles is considered where each vehicle is using the vehicle in the front as a reference point. The coupled motion stability of the formation is analyzed by linearization. It is shown that under the assumed dynamics, guidance, and control laws, the stability properties of the system decoupled into individual vehicles. This makes it possible to obtain exact analytical results that can be used in design. Parametric runs and sensitivity analysis studies show the effect of main vehicle geometric parameters on formation control and motion stability.

THIS PAGE INTENTIONALLY LEFT BLANK

TABLE OF CONTENTS

THIS PAGE INTENTIONALLY LEFT BLANK

LIST OF FIGURES

THIS PAGE INTENTIONALLY LEFT BLANK

LIST OF TABLES

THIS PAGE INTENTIONALLY LEFT BLANK

ACKNOWLEDGMENTS

Many thanks are due to those who helped and encouraged me to finish this thesis.

First, I would like to give my sincere gratitude to my advisor, Professor Fotis A. Papoulias, without whom the writing of this thesis would not have been possible. I would also like to express my deepest thanks to my co-advisor Professor Oleg Yakimenko.

I would like to thank my friends here in Monterey who helped me feel at home over the past two years. Particularly, I would like to thank Chris Daskam, Jason Downs, Russell Canty and Grant Bryan for the help they always offered at difficult times and for their enjoyable friendship.

Finally, my biggest thanks go to my family. Their constant understanding and support is the source of my strength and courage. I am especially grateful to my lovely wife, Ilkin Ece Babaoglu, for her patience and love and for the happiness she brings into my life every day.

THIS PAGE INTENTIONALLY LEFT BLANK

I. INTRODUCTION

A. MOTIVATION

Unmanned vehicles become more and more sophisticated every day. This increase in sophistication is accompanied by an increase in requirements and missions they are called upon to complete. As a result, it is often required that they operate in a formation with specific goals to accomplish. As the vehicles operate in formations, it is possible that motion stability may be an issue. In many areas, such as land vehicles, it has been found that a certain type of instability, most notably string instability, may develop when vehicles are travelling in a formation. Therefore, we need to investigate the stability of motion of unmanned surface vehicles as they maneuver in the horizontal plane. We need to establish if they lose their stability and under what conditions, so that we can design or operate vehicles in a more efficient and effective manner.

B. BACKGROUND

1. Background and Literature Review

Mathematical models based on dynamic characteristics are both necessary and important in order to formulate response and stability analysis problems for marine surface vehicles. Different coordinates systems are adopted in order to investigate the maneuverability of a marine surface vehicle. Typically, two coordinates are employed for modeling the three degrees of freedom for vehicle motion control, as described in Figure 1 [2, 7, 9]. One is the earth-fixed coordinate system $x_0 y_0 z_0$, and the other is the body-fixed coordinate system xyz which moves together with the vessel.

There are several mathematical models in use for control system design and analysis. They are generally linear models or simplified nonlinear models. Nomoto's model is a relatively simple but effective model for course keeping control and autopilot design [2, 7, 9, 12]. Based on Nomoto's model, a state feedback control law can be coupled with a line of sight guidance law to provide path control as explained in [1].

In the work reported in [2], an instability phenomenon arising from mis-coordination of guidance and control laws for marine surface vehicles moving in a platoon was studied. Moreover, the question of how it is possible for ships traveling in formation to exhibit the phenomenon of string instability was answered.

One of the necessary tasks for all studies involving vehicle maneuvering is an estimate of the coefficients in the equations of motion. In this thesis we use an empirical Maneuvering Prediction Program which offers two main options. One is the Linear Evaluation which implements the methods proposed in [3] for the assessment of course stability and turning ability. The other is Turning Prediction which implements the multiple linear regression equations presented in [4] for the estimation of turning circle characteristics. In the Linear Evaluation option, water depth corrections were added by using regression analysis formulas based on the data presented in [5]. In addition, the trim corrections used in the above program were presented in [6]. These trim corrections are used primarily for velocity derivatives.

2. Thesis Overview

The objectives of this thesis are as follows:

First, we want to formulate the guidance and control problem in the horizontal plane for a string of unmanned vehicles and establish the conditions for stability. In addition, we want to see how these conditions relate to the conditions for directional stability of a single vehicle.

Second, we want to investigate the relationship between such stability conditions and fundamental geometric parameters of the vehicle. Such relationships, if they can be derived, will be very useful in preliminary design phases.

This thesis is organized as follows:

Chapter II contains the problem formulation. We present an overview of the equations of motion for marine vehicles in the horizontal plane with a set of assumptions as they pertain to this study. A reduction of the order of the equations of motion then follows. This reduction forms the basis for the development of control and guidance laws

for one and for a string of vehicles. The final set of equations that model the behavior of a string of vehicles in a string formation is developed and presented in this chapter.

Chapter III presents the stability analysis of the final set of equations developed in Chapter 2. Stability is based on a linearized set of equations. We form the characteristic equation of the system, and we apply Routh's criterion in order to derive the final set of stability conditions. These are presented in terms of operational and control design parameters.

Chapter IV presents a set of parametric analysis results. We express the previously derived stability conditions in terms of a number of physical parameters of the vehicles. This way a designer can incorporate motion and formation control considerations into the early stages of design or operation and, therefore, better match vehicle capabilities to operational requirements.

Chapter V summarizes the conclusions from this study and offers recommendations for further research.

THIS PAGE INTENTIONALLY LEFT BLANK

II. PROBLEM FORMULATION

A. INTRODUCTION

A mathematical model for the problem of path keeping in the horizontal plane is derived in this chapter. The objective of path keeping in this context is to drive the surface marine vessel to follow a commanded path. Starting with the equations of motion for a marine surface vessel during maneuvering in a horizontal plane, we derive the basic turning dynamics of the vessel. By using these turning dynamics equations, we suggest a control law for the autopilot, which in coordination with an appropriate guidance scheme stabilizes the vessel to a commanded heading angle ψ_C capable of restoring the vessel to the commanded path. Finally, we arrive at the system of equations that describes the behavior of three vessels moving in a formation, and according to the combined guidance and control law.

B. EQUATIONS OF MOTION

The rapid advances in computer technology have resulted in successful applications in ship engineering. Hence, methods of computer simulation using the mathematical models become increasingly important. In the design process, computer simulation and analysis provide a convenient tool for predicting ship maneuverability. Development of the equations describing the maneuvering motion is one of the requirements for applying methods of computer simulation and analysis, and this development process is presented in the following sections.

1. Coordinate Systems

The vessel is considered to be a rigid body with only three degrees of freedom—surge, sway and yaw—and which maneuvers in the horizontal plane. The other three degrees of freedom—roll, pitch and heave—are neglected and are not considered in this study [7], see Figure 1. Two coordinate systems are adopted in order to investigate the maneuverability of a marine surface vessel. One is the earth-fixed coordinate system $x_0 y_0 z_0$, and the other is the body-fixed coordinate system xyz which moves together with

the vessel, see Figure 1. The x_0y_0 plane and the xy plane lie on the free surface, with the x_0 axis pointing to the direction of the original course of the vessel, while the z_0 axis and the z axis point upwards vertically. The angle between the x_0 axis and x axis is defined as the yaw angle ψ. When the maneuvering motion starts, the two coordinate systems coincide with each other. After any amount of time, the position of the vessel is determined by the coordinates x_{0G} and y_{0G} of the vessel center of gravity in the earth-fixed coordinate system, and the orientation of the vessel is determined by the yaw angle ψ.

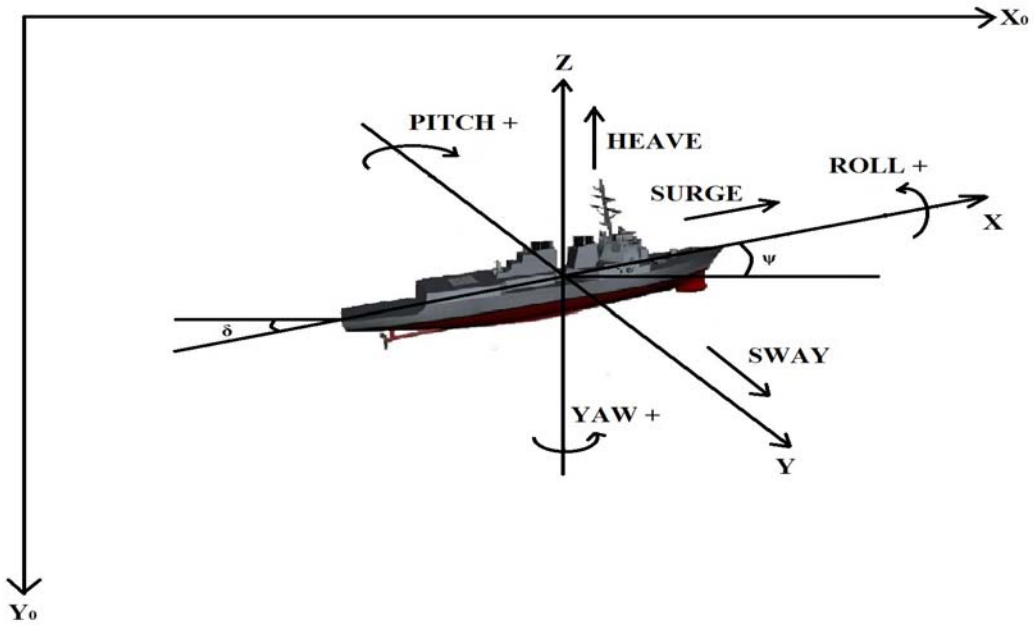

Figure 1. The earth-fixed coordinate system and the body-fixed coordinate system. After [8].

The vessel maneuvering motion in the horizontal plane can be described by using Newton's second law and the yaw rate about the z axis which is defined as $r = \dot{\psi}$. In the earth-fixed coordinate system, the equations of motion are as follows:

$$\begin{aligned} m\ddot{x}_0 &= X_0 \\ m\ddot{y}_0 &= Y_0 \\ I_z\ddot{\psi} &= N \end{aligned} \qquad (1)$$

where X_0 and Y_0 are the components of total force acting on the vessel in the directions of x_0 axis and y_0 axis, respectively; N is the external moment about the z axis; m is the vessel's mass; I_z is the moment of inertia of the ship about z axis; $\ddot{x}_0$ and $\ddot{y}_0$ are the accelerations in the directions of x_0 axis and y_0 axis, respectively.

Equations of motion in the earth-fixed coordinate system can be expressed with respect to a body-fixed coordinate system. We fix the origin of the body-fixed coordinate system lying on the center of gravity,

$$\begin{aligned} x_{0G} + x\cos\psi - y\sin\psi &= x_0 \\ y_{0G} + x\sin\psi + y\cos\psi &= y_0 \\ z &= z_0 \end{aligned} \tag{2}$$

Replacing the components of total force in the directions of x axis and y axis by X and Y, and the components of vessel speed in the directions of x axis and y axis by u_G and v_G in Equation (2), we obtain

$$\begin{aligned} X_0\cos\psi + Y_0\sin\psi &= X \\ -X_0\sin\psi + Y_0\cos\psi &= Y \end{aligned} \tag{3}$$

$$\begin{aligned} u_G\cos\psi - v_G\sin\psi &= \dot{x}_{0G} \\ u_G\sin\psi + v_G\cos\psi &= \dot{y}_{0G} \end{aligned} \tag{4}$$

By differentiation of Equation (4) with respect to time we get

$$\begin{aligned} \dot{u}_G\cos\psi - u_G\dot{\psi}\sin\psi - \dot{v}_G\sin\psi - v_G\dot{\psi}\cos\psi &= \ddot{x}_{0G} \\ \dot{u}_G\sin\psi + u_G\dot{\psi}\cos\psi + \dot{v}_G\cos\psi - v_G\dot{\psi}\sin\psi &= \ddot{y}_{0G} \end{aligned} \tag{5}$$

Substituting Equations (1) and (5) into Equation (3), we obtain the equations of motion in the body-fixed coordinate system, with the original of the system lying on the ship center of gravity, as

$$\begin{aligned} m\dot{u}_G - mv_G r &= X \\ m\dot{v}_G + mu_G r &= Y \\ I_z\dot{r} &= N \end{aligned} \tag{6}$$

In practice, it is more convenient when the original of the body-fixed coordinate system lies at amidships instead of the center of gravity, since the latter depends on the

loading condition of the vehicle. Assuming that the ship is symmetrical about its longitudinal center plane, the center of gravity has the coordinates $(x_G, 0, z_G)$ in the body-fixed coordinate system with the original lying at amidships. With this information in mind, the components of vessel speed at the center of gravity, u_G and v_G can be expressed as follows:

$$\begin{aligned} u_G &= u \\ v_G &= v + x_G\dot{\psi} \\ I_z &= I_{zG} + mx_G^2 \end{aligned} \tag{7}$$

Hence, we obtain the equations of motion in the body-fixed coordinate system with the original lying at amidships as [9]

$$\begin{aligned} m(\dot{u} - vr - x_G r^2) &= X \\ m(\dot{v} + ur + x_G\dot{r}) &= Y \\ I_Z\dot{r} + mx_G(\dot{v} + ur) &= N \end{aligned} \tag{8}$$

where u and v are the surge and sway velocity, respectively; and x_G is the x-coordinate of the center of mass G.

2. Hydrodynamic Forces

In Equation (8), the components of total force and moment acting on the surface marine vessel are designated as X, Y and N. These force and moment components involve the hydrodynamic force and moment due to different environmental force and moment such as surrounding water forces, wind forces, wave forces, rudder and thruster forces, etc. We will assume no other environmental forces.

There are two different approaches to presenting the hydrodynamic force and moment. One of them was proposed by Prof. Martin A. Abkowitz, who was the Director of the MIT Ship Model Towing Tank.

Prof. Abkowitz used the Taylor expansion series to express the hydrodynamic force and moment. The hydrodynamic force and moment are expressed as the following form [7]

$$
\begin{aligned}
X &= X(u, v, r, \dot{u}, \dot{v}, \dot{r}, \delta) \\
Y &= Y(u, v, r, \dot{u}, \dot{v}, \dot{r}, \delta) \\
N &= N(u, v, r, \dot{u}, \dot{v}, \dot{r}, \delta)
\end{aligned} \tag{9}
$$

These equations were then expanded in Taylor series about the initial steady state of forward motion with constant speed, $u_0 = U, v_0 = 0, r_0 = 0, \dot{u}_0 = 0, \dot{v}_0 = 0, \dot{r}_0 = 0, \delta_0 = 0$. This results in [7]

$$
\begin{aligned}
X &= X_0 + \frac{\partial X}{\partial u}(u-U) + \frac{\partial X}{\partial v}v + \frac{\partial X}{\partial r}r + \frac{\partial X}{\partial \dot{u}}\dot{u} + \frac{\partial X}{\partial \dot{v}}\dot{v} + \frac{\partial X}{\partial \dot{r}}\dot{r} + \frac{\partial X}{\partial \delta}\delta \\
&\quad + \frac{1}{2!}\left[\frac{\partial}{\partial u}(u-U) + \frac{\partial}{\partial v}v + \frac{\partial}{\partial r}r + \frac{\partial}{\partial \dot{u}}\dot{u} + \frac{\partial}{\partial \dot{v}}\dot{v} + \frac{\partial}{\partial \dot{r}}\dot{r} + \frac{\partial}{\partial \delta}\delta\right]^2 X \\
&\quad + \ldots + \frac{1}{n!}\left[\frac{\partial}{\partial u}(u-U) + \frac{\partial}{\partial v}v + \frac{\partial}{\partial r}r + \frac{\partial}{\partial \dot{u}}\dot{u} + \frac{\partial}{\partial \dot{v}}\dot{v} + \frac{\partial}{\partial \dot{r}}\dot{r} + \frac{\partial}{\partial \delta}\delta\right]^n X + \ldots \\
Y &= Y_0 + \frac{\partial Y}{\partial u}(u-U) + \frac{\partial Y}{\partial v}v + \frac{\partial Y}{\partial r}r + \frac{\partial Y}{\partial \dot{u}}\dot{u} + \frac{\partial Y}{\partial \dot{v}}\dot{v} + \frac{\partial Y}{\partial \dot{r}}\dot{r} + \frac{\partial Y}{\partial \delta}\delta \\
&\quad + \frac{1}{2!}\left[\frac{\partial}{\partial u}(u-U) + \frac{\partial}{\partial v}v + \frac{\partial}{\partial r}r + \frac{\partial}{\partial \dot{u}}\dot{u} + \frac{\partial}{\partial \dot{v}}\dot{v} + \frac{\partial}{\partial \dot{r}}\dot{r} + \frac{\partial}{\partial \delta}\delta\right]^2 Y \\
&\quad + \ldots + \frac{1}{n!}\left[\frac{\partial}{\partial u}(u-U) + \frac{\partial}{\partial v}v + \frac{\partial}{\partial r}r + \frac{\partial}{\partial \dot{u}}\dot{u} + \frac{\partial}{\partial \dot{v}}\dot{v} + \frac{\partial}{\partial \dot{r}}\dot{r} + \frac{\partial}{\partial \delta}\delta\right]^n Y + \ldots \\
N &= N_0 + \frac{\partial N}{\partial u}(u-U) + \frac{\partial N}{\partial v}v + \frac{\partial N}{\partial r}r + \frac{\partial N}{\partial \dot{u}}\dot{u} + \frac{\partial N}{\partial \dot{v}}\dot{v} + \frac{\partial N}{\partial \dot{r}}\dot{r} + \frac{\partial N}{\partial \delta}\delta \\
&\quad + \frac{1}{2!}\left[\frac{\partial}{\partial u}(u-U) + \frac{\partial}{\partial v}v + \frac{\partial}{\partial r}r + \frac{\partial}{\partial \dot{u}}\dot{u} + \frac{\partial}{\partial \dot{v}}\dot{v} + \frac{\partial}{\partial \dot{r}}\dot{r} + \frac{\partial}{\partial \delta}\delta\right]^2 N \\
&\quad + \ldots + \frac{1}{n!}\left[\frac{\partial}{\partial u}(u-U) + \frac{\partial}{\partial v}v + \frac{\partial}{\partial r}r + \frac{\partial}{\partial \dot{u}}\dot{u} + \frac{\partial}{\partial \dot{v}}\dot{v} + \frac{\partial}{\partial \dot{r}}\dot{r} + \frac{\partial}{\partial \delta}\delta\right]^n N + \ldots
\end{aligned} \tag{10}
$$

where $u_0 = U, v_0 = 0, r_0 = 0, \dot{u}_0 = 0, \dot{v}_0 = 0, \dot{r}_0 = 0, \delta_0 = 0$.

The equations of maneuvering motion are then derived by substituting Equation (10) into Equation (8).

The other approach to define the hydrodynamic force and moment was derived by the Japanese research group named Maneuvering Mathematical Modeling Group (MMMG). This approach consists of the hydrodynamic force and moment acting on the

ship hull, propeller, and rudder, as well as the interaction between them. This expression can be described as in Equation (11).

$$\begin{aligned} X &= X_H + X_P + X_R \\ Y &= Y_H + Y_P + Y_R \\ N &= N_H + N_P + N_R \end{aligned} \tag{11}$$

where the subscripts H, P and R refer to the hull, the propeller and the rudder, respectively.

By plugging Equation (11) into Equation (8), we obtain the equations of ship maneuvering motion. This kind of equation is called the MMMG model. If the components of the MMMG model are expressed in Taylor series expansions and truncated to first order, the two models are identical.

C. LINEAR EQUATIONS OF MOTION

As mentioned before, the mathematical models generated by using equations of a marine vessel during maneuvering can be used for simulation and analysis. This helps to predict ship maneuverability. In order to analyze ship maneuverability, we can use a simplified or linear set of equations.

The force and moment include hydrodynamic derivatives as coefficients. Assuming that, during ordinary maneuvering motions, the changes in velocities and accelerations $\Delta u = u - U, \Delta v = v, \Delta r = r, \Delta \dot{u} = \dot{u}, \Delta \dot{v} = \dot{v}, \Delta \dot{r} = \dot{r}$ and the rudder angle δ are small, the higher order terms in the series in Equation (10) can be ignored. Hence, we can derive the linear equations of motion as

$$\begin{aligned} m(\dot{u} - vr - x_G r^2) &= X_0 + X_u(u-U) + X_v v + X_r r + X_{\dot{u}}\dot{u} + X_{\dot{v}}\dot{v} + X_{\dot{r}}\dot{r} + X_\delta \delta \\ m(\dot{v} + ur + x_G \dot{r}) &= Y_0 + Y_u(u-U) + Y_v v + Y_r r + Y_{\dot{u}}\dot{u} + Y_{\dot{v}}\dot{v} + Y_{\dot{r}}\dot{r} + Y_\delta \delta \\ I_Z \dot{r} + m x_G(\dot{v} + ur) &= N_0 + N_u(u-U) + N_v v + N_r r + N_{\dot{u}}\dot{u} + N_{\dot{v}}\dot{v} + N_{\dot{r}}\dot{r} + N_\delta \delta \end{aligned} \tag{12}$$

Assuming $ur = (u - U + U)r = (u-U)r + Ur \approx Ur$, $X_0 = 0, Y_0 = 0, N_0 = 0$ and neglecting the terms $vr, x_G r^2$ in Equation (12) results in

$$
\begin{aligned}
m\dot{u} &= X_u(u-U) + X_v v + X_r r + X_{\dot{u}}\dot{u} + X_{\dot{v}}\dot{v} + X_{\dot{r}}\dot{r} + X_\delta \delta \\
m(\dot{v} + Ur + x_G\dot{r}) &= Y_u(u-U) + Y_v v + Y_r r + Y_{\dot{u}}\dot{u} + Y_{\dot{v}}\dot{v} + Y_{\dot{r}}\dot{r} + Y_\delta \delta \\
I_Z\dot{r} + mx_G(\dot{v} + Ur) &= N_u(u-U) + N_v v + N_r r + N_{\dot{u}}\dot{u} + N_{\dot{v}}\dot{v} + N_{\dot{r}}\dot{r} + N_\delta \delta
\end{aligned} \tag{13}
$$

For ease of understanding, we can take into account the port-starboard symmetry of the vessel. Under this assumption, many of the linear hydrodynamic derivatives, such as, $X_v, X_r, X_{\dot{v}}, X_{\dot{r}}, X_\delta, Y_u, Y_{\dot{u}}, N_u$ and $N_{\dot{u}}$ vanish. Hence, the linear equations of motion can be simplified as

$$
\begin{aligned}
(m - Y_{\dot{v}})\dot{v} - (Y_{\dot{r}} - mx_G)\dot{r} &= Y_v v + (Y_r - mu)r + Y_\delta \delta \\
(I_Z - N_{\dot{r}})\dot{r} - (N_{\dot{v}} - mx_G)\dot{v} &= N_v v + (N_r - mx_G u)r + N_\delta \delta
\end{aligned} \tag{14}
$$

Non-dimensionalization of the equations of motion in terms of water density ρ, vessel length L, and nominal velocity U can be expressed in the form [9]

$$
\begin{aligned}
(m - Y_{\dot{v}})\dot{v} - (Y_{\dot{r}} - mx_G)\dot{r} &= Y_v v + (Y_r - m)r + Y_\delta \delta \\
(I_Z - N_{\dot{r}})\dot{r} - (N_{\dot{v}} - mx_G)\dot{v} &= N_v v + (N_r - mx_G)r + N_\delta \delta
\end{aligned} \tag{15}
$$

D. AUTOPILOT CONTROL LAW (NOMOTO MODEL)

Nomoto's first order model is mainly used to describe the fundamental turning dynamics of ship motions or to design automatic control devices such as autopilots. In this section, we will continue working on dimensionless linear equations of motion. Using these equations, we will finally obtain Nomoto's first order model.

1. Turning Dynamics

Solving Equation (15) for $\dot{v}$ and v, we get

$$
\begin{aligned}
v &= \frac{(m - Y_{\dot{v}})\dot{v}\left[N_\delta\delta - (mx_G U - N_r)r - (I_z - N_{\dot{r}})\dot{r}\right] - (mx_G - N_{\dot{v}})\left[Y_\delta\delta - (mU - Y_r)r - (mx_G - Y_{\dot{r}})\dot{r}\right]}{Y_v(mx_G - N_{\dot{v}}) - N_v(m - Y_{\dot{v}})} \\
\dot{v} &= \frac{Y_v\left[N_\delta\delta - (mx_G U - N_r)r - (I_z - N_{\dot{r}})\dot{r}\right] - N_v\left[Y_\delta\delta - (mU - Y_r)r - (mx_G - Y_{\dot{r}})\dot{r}\right]}{Y_v(mx_G - N_{\dot{v}}) - N_v(m - Y_{\dot{v}})}
\end{aligned} \tag{16}
$$

Differentiating the first equation of Equation (16) with respect to time and setting the result equal to the second equation, we obtain the basic turning dynamics of a marine surface vessel [9]

$$
\begin{aligned}
T_1T_2\ddot{r} + (T_1 + T_2)\dot{r} + r &= K\delta + KT_3\dot{\delta} \\
T_1T_2\ddot{v} + (T_1 + T_2)\dot{v} + v &= K_v\delta + K_vT_4\dot{\delta}
\end{aligned}
\tag{17}
$$

where

$$
T_1T_2 = \frac{(Y_{\dot{v}} - m)(N_{\dot{r}} - I_z) - (Y_{\dot{r}} - mx_G)(N_{\dot{v}} - mx_G)}{Y_v(N_r - mx_GU) - N_v(Y_r - mU)}
$$

$$
T_1 + T_2 = \frac{(Y_{\dot{v}} - m)(N_r - mx_GU) + Y_v(N_{\dot{r}} - I_z)}{Y_v(N_r - mx_GU) - N_v(Y_r - mU)} - \frac{(Y_{\dot{r}} - mx_G)N_v + (Y_r - mU)(N_{\dot{v}} - mx_G)}{Y_v(N_r - mx_GU) - N_v(Y_r - mU)}
$$

$$
T_3 = \frac{Y_\delta(N_{\dot{v}} - mx_G) - N_\delta(Y_{\dot{v}} - m)}{Y_\delta N_v - N_\delta Y_v}
$$

$$
T_4 = \frac{Y_\delta(N_{\dot{r}} - I_z) - N_\delta(Y_{\dot{r}} - mx_G)}{Y_\delta(N_r - mx_GU) - N_\delta(Y_r - mU)}
$$

$$
K = \frac{Y_\delta N_v - N_\delta Y_v}{Y_v(N_r - mx_GU) - N_v(Y_r - mU)}
$$

$$
-K_v = \frac{Y_\delta(N_r - mx_GU) - N_\delta(Y_r - mU)}{Y_v(N_r - mx_GU) - N_v(Y_r - mU)}
$$

The first equation of Equation (17) expresses the relationship between the ship turning rate and the rudder angle.

We can further assume that $x_G \approx 0, Y_r \approx 0, Y_{\dot{r}} \approx 0, N_v \approx 0, N_{\dot{v}} \approx 0$. Strictly speaking, such equations would be true for a fore/aft symmetric vehicle. It has been shown, however, that a reasonable degree of accuracy is maintained even for vehicles that are not symmetric. By using these, we can obtain

$$
\begin{aligned}
K &\approx -\frac{N_\delta}{N_r} \\
T_1 + T_2 &\approx -\frac{I_z - N_{\dot{r}}}{N_r} - \frac{m - Y_{\dot{v}}}{Y_v} \\
T_3 &\approx -\frac{m - Y_{\dot{v}}}{Y_v} \\
T_1 + T_2 - T_3 &\approx -\frac{I_z - N_{\dot{r}}}{N_r}
\end{aligned}
\tag{18}
$$

From the second equation of Equation (14) we get

$$
-\frac{I_z - N_{\dot{r}}}{N_r}\dot{r} + r = -\frac{N_\delta}{N_r}\delta \tag{19}
$$

By using $T = T_1 + T_2 - T_3$ and plugging Equation (18) into Equation (19), the first of Equation (17) can be further reduced to a first order model

$$T\dot{r} + r = K\delta \tag{20}$$

Equation (20) was firstly derived by Nomoto by using the method of Laplace Transformation. Therefore, this first order model is called the Nomoto model. In this model, K and T are called the maneuverability indexes, and they have explicit relations with maneuvering characteristics.

Equation (18) can be expressed as in the form [1]

$$\dot{r} + \frac{1}{T}r = \frac{K}{T}\delta \text{ or } \dot{r} = ar + b\delta \tag{21}$$

where the two parameters are

$a = -\frac{1}{T}, b = \frac{K}{T}$.

2. Control Law

A linear heading feedback control law based on Equation (21) has the form [1]

$$\delta_0 = k_1(\psi - \psi_c) + k_2 r \tag{22}$$

where ψ_c is the commanded heading angle.

By using $\dot{\psi} = r$, the system characteristic equation is obtained from Equation (21) and Equation (22). The system characteristic equation is as follows

$$s^2 - (a + bk_2)s - bk_1 = 0 \tag{23}$$

The controller gains can be computed from the comparison of the second order system equation as follows:

$$s^2 + 2\zeta\omega_n s + \omega_n{}^2 = 0 \tag{24}$$

$$k_1 = -\frac{\omega_n^2}{b}, k_2 = -\frac{a + 2\zeta\omega_n}{b} \tag{25}$$

The commanded rudder angle is given by [1]

$$\delta = \delta_{sat} \tanh(\frac{\delta_0}{\delta_{sat}}) \tag{26}$$

where δ_{sat} is the saturation limit and typically set at 0.4 radians, δ_0 is the slope of the function at zero, and it is given by Equation (22).

E. EQUATIONS FOR GUIDANCE

The guidance scheme is described in [1] and is basically illustrated in Figure 2. In Figure 2, the vessel located at *(x,y)* changes its direction toward a target point *D* which is located ahead of the vessel at a distance *d* on the vessel's nominal path. According to [1], pure pursuit guidance is achieved by commanding a heading angle ψ_c equal to the line of sight angle σ

$$\psi_C = -\tan^{-1}\frac{y}{d} \tag{27}$$

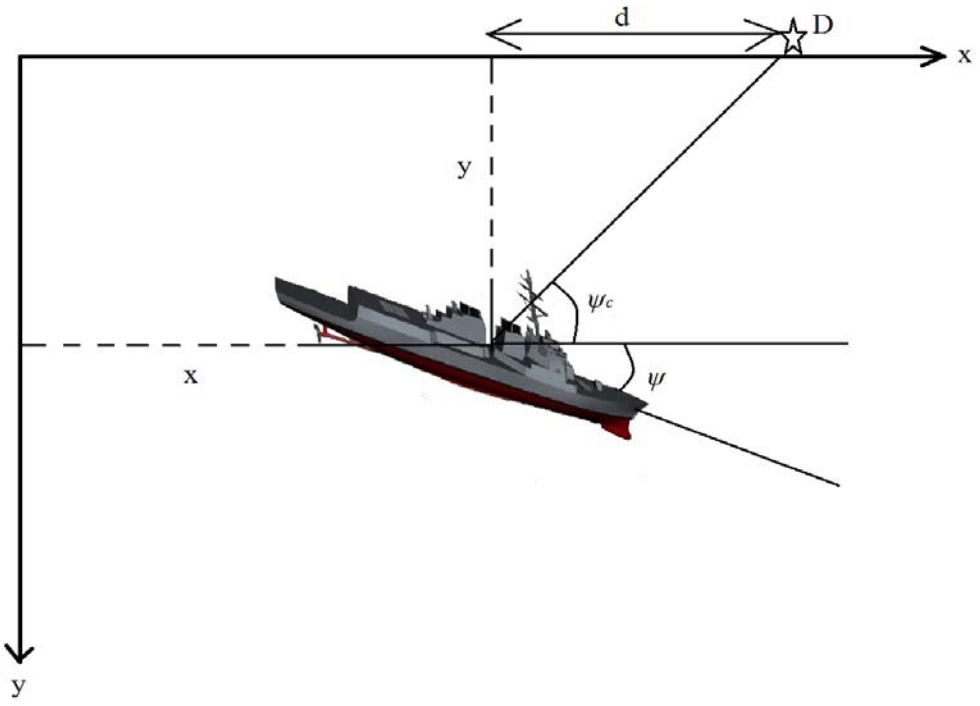

Figure 2. The Line of Sight Guidance Scheme. After [8]

The guidance law is based on the inertial deviation rate from the commanded path [1]

$$\dot{y} = \sin\psi \tag{28}$$

It is worthwhile to note that guidance law would be globally asymptotically stable provided that the commanded heading angle ψ_c is equal to the vessel's heading angle ψ. Moreover, the commanded heading angle ψ_c is a function of the vessel's position and the distance *d*. Therefore, the smaller the value of distance d, the faster the guidance law response is. The autopilot has a limited reaction time according to the specified natural frequency ω_n and damping ratio ζ. Thus, this parameter *d* must be chosen properly for the desired response to be achieved [1].

F. COMBINED GUIDANCE AND CONTROL LAW

In this section, the combined guidance and control law is derived. The combined guidance and control law describes the behavior of a vessel that has deviated from the commanded straight-line path and attempts to return by following a target point *D* (see Figure 2). Then, we expand this scenario for three vessels moving in a string or series formation.

1. One Vessel

Substituting the commanded heading angle ψ_c defined in Equation (27) into the control law, Equation (22), we obtain

$$\delta_0 = k_1(\psi + \tan^{-1}\frac{y}{d}) + k_2 r \tag{29}$$

For very small commanded heading angle ψ_c, Equation (29) can be further reduced to

$$\delta_0 = k_1(\psi + \frac{y}{d}) + k_2 r \tag{30}$$

This is simply the linearized form of (29). Combining Equation (21) with Equations (26) and (30) yields

$$\dot{r} = ar + b\delta_{sat}\tanh(\frac{1}{\delta_{sat}}k_1(\psi + \frac{y}{d}) + k_2 r) \tag{31}$$

The complete system of equations is given by

$$\dot{\psi} = r$$
$$\dot{r} = ar + b\delta_{sat} \tanh(\frac{1}{\delta_{sat}} k_1(\psi + \frac{y}{d}) + k_2 r)$$
$$\dot{y} = \sin\psi \tag{32}$$

In linearized form we have,

$$\dot{\psi} = r$$
$$\dot{r} = ar + b(k_1(\psi + \frac{y}{d}) + k_2 r)$$
$$\dot{y} = \psi \tag{33}$$

Equations (33) can be expressed in matrix form as

$$\dot{x} = Ax \tag{34}$$

where $x = [\psi, r, y]^T$ and $A = \begin{bmatrix} 0 & 1 & 0 \\ bk_1 & a + bk_2 & \frac{bk_1}{d} \\ 1 & 0 & 0 \end{bmatrix}$

The controller gains in Equation (25) can be re-defined as

$$bk_1 = -\omega_n^2$$
$$a + bk_2 = -2\zeta\omega_n \tag{35}$$

Consequently matrix A is written as

$$A = \begin{bmatrix} 0 & 1 & 0 \\ -\omega_n^2 & -2\zeta\omega_n & -\frac{\omega_n^2}{d} \\ 1 & 0 & 0 \end{bmatrix} \tag{36}$$

2. Three Vessels

Now we can expand the previous concept for the case of three vessels moving in a string or serial formation. In this case, the first vessel attempts to direct its longitudinal axis toward a target point D, whereas the second vessel points its longitudinal axis toward the first one and so on (see Figure 3). In this consideration, d_1 is the distance between the target point D and the first vessel d_2 is the distance between the first and the second vessel; and d_3 is the distance between the last two vessels always measured on the commanded path.

The system of equations for the first vessel is

$$\dot{\psi}_1 = r_1$$
$$\dot{r}_1 = a_1 r_1 + b_1 (k_{11} (\psi_1 + \frac{y_1}{d_1}) + k_{21} r_1)$$
$$\dot{y}_1 = \psi_1 \qquad (37)$$

For the second vessel, they become

$$\dot{\psi}_2 = r_2$$
$$\dot{r}_2 = a_2 r_2 + b_2 (k_{12} (\psi_2 + \frac{y_2 - y_1}{d_2}) + k_{22} r_2)$$
$$\dot{y}_2 = \psi_2 \qquad (38)$$

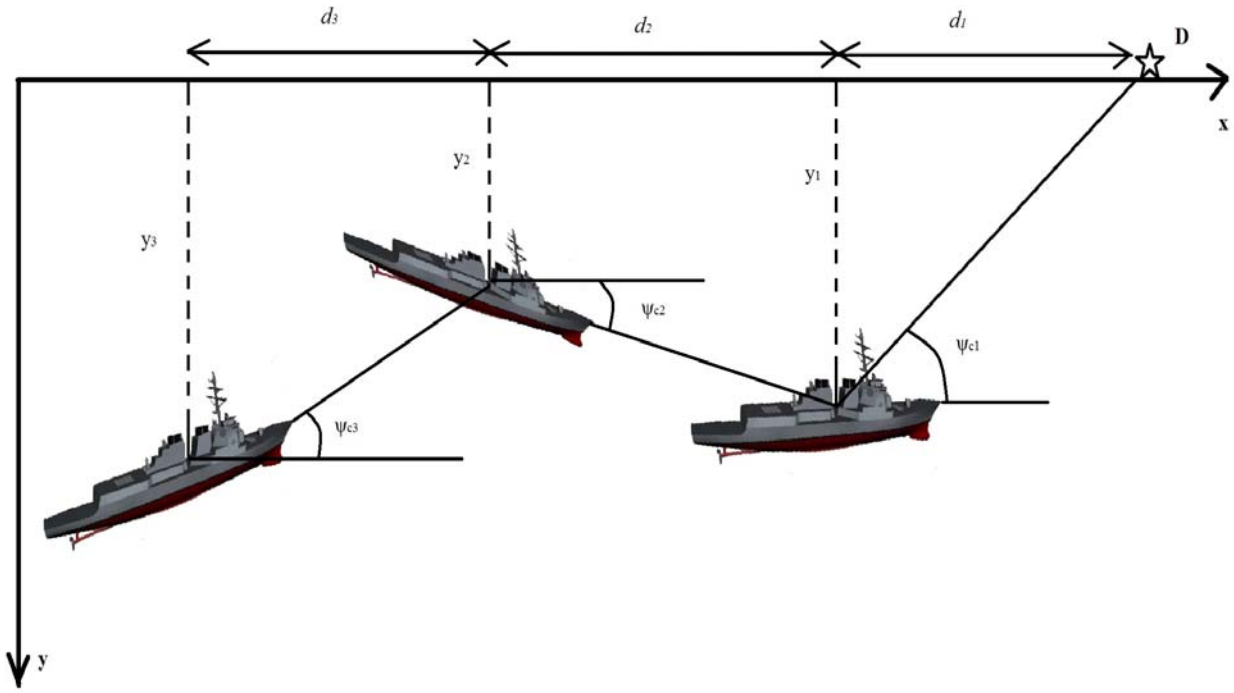

Figure 3. Three vessels in a formation, which have deviated from the commanded straight line path (x axis). After [8]

Finally, the system of equations for the third vessel is

$$\dot{\psi}_3 = r_3$$
$$\dot{r}_3 = a_3 r_3 + b_3(k_{23}(\psi_3 + \frac{y_3 - y_2}{d_3}) + k_{33} r_3) \tag{39}$$
$$\dot{y}_3 = \psi_3$$

or

$$\dot{x} = Ax \tag{40}$$

where

$x = [\psi_1, r_1, y_1, \psi_2, r_2, y_2, \psi_3, r_3, y_3]$ and the system matrix is given by

$$A = \begin{bmatrix} 0 & 1 & 0 & 0 & 0 & 0 & 0 & 0 & 0 \\ -\omega_{n_1}{}^2 & -2\zeta_1\omega_{n_1} & \frac{-\omega_{n_1}{}^2}{d_1} & 0 & 0 & 0 & 0 & 0 & 0 \\ 1 & 0 & 0 & 0 & 0 & 0 & 0 & 0 & 0 \\ 0 & 0 & 0 & 0 & 1 & 0 & 0 & 0 & 0 \\ 0 & 0 & \frac{\omega_{n_2}{}^2}{d_2} & -\omega_{n_2}{}^2 & -2\zeta_2\omega_{n_2} & \frac{-\omega_{n_2}{}^2}{d_2} & 0 & 0 & 0 \\ 0 & 0 & 0 & 1 & 0 & 0 & 0 & 0 & 0 \\ 0 & 0 & 0 & 0 & 0 & 0 & 0 & 1 & 0 \\ 0 & 0 & 0 & 0 & 0 & \frac{\omega_{n_3}{}^2}{d_3} & -\omega_{n_3}{}^2 & -2\zeta_3\omega_{n_3} & \frac{-\omega_{n_3}{}^2}{d_3} \\ 0 & 0 & 0 & 0 & 0 & 0 & 1 & 0 & 0 \end{bmatrix} \tag{41}$$

III. STABILITY ANALYSIS

A. INTRODUCTION

In this chapter, the problem of stability for one vessel is initially studied. Then, the problem of stability for three vessels moving in a formation with constant speed on a straight-line commanded path (trivial equilibrium solution characterized by $\psi=r=y=0$) is analyzed. The solution described here builds on and extends previous work in [2]. All vessels can deviate from the commanded path due to external disturbances such as a wave or another external disturbance or change in mission requirements. This is translated to some non-zero initial conditions. The system is prone to instability phenomena due to incorrect coordination of guidance and control laws. Specific criteria for stability and conclusions about the effect of damping ratio ζ and natural frequency ω_n are drawn.

B. STABILITY OF ONE VESSEL

For the case of one vessel, we have already referred to the combined guidance and control law, Equation (34), and the matrix A is

$$A=\begin{bmatrix} 0 & 1 & 0 \\ -\omega_n^{\,2} & -2\zeta\omega_n & -\dfrac{\omega_n^{\,2}}{d} \\ 1 & 0 & 0 \end{bmatrix} \tag{42}$$

Local stability properties can then be established by the eigenvalues of matrix A. The characteristic equation of A is

$$\lambda^3+2\zeta\omega_n\lambda^2+\omega_n^{\,2}\lambda+\frac{\omega_n^{\,2}}{d}=0 \tag{43}$$

We can observe that if we neglect the constant term $\dfrac{\omega_n^{\,2}}{d}$ from Equation (42) (i.e., $d\to\infty$ or the guidance law is eliminated), Equation (43) reduces to Equation (24) (i.e.,

the characteristic equation when control law stabilizes the vessel to any commanded heading angle ψ_c without the presence of the guidance law).

Applying Routh's criterion to Equation (43) we get

$$2\zeta\omega_n{}^3 - \frac{\omega_n{}^2}{d} > 0 \Rightarrow d > \frac{1}{2\zeta\omega_n} \qquad \text{or} \qquad d_{critical} = \frac{1}{2\zeta\omega_n} \quad (44)$$

For $d > \frac{1}{2\zeta\omega_n}$ all eigenvalues of A have negative real parts, and the combined guidance and control law provides stability (i.e., the vessel follows the commanded path).

On the other hand, we already referred to the controller gains, as in Equation (25). Using Equation (25) we obtain

$$\omega_n = -\sqrt{k_1 b} \quad (45)$$

$$\zeta = \frac{k_2 b + a}{2\omega_n} \quad (46)$$

Substituting Equation (45) and (46) into Equation (44), $d_{critical}$ can be expressed in the form

$$d_{critical} = \frac{1}{k_2 b + a} \quad (47)$$

Equation (47) proves that $d_{critical}$ depends only on k_2 and maneuverability indexes, and it does not depend on k_1. In other words, we see that the critical distance for stability of the combined law is a function of the derivative gain of the vehicle control law, an observation which had escaped previous studies. We conclude that the overall stability of the system depends then on the speed of response of the vehicle to the rate of change of its commanded heading angle. A vehicle that has a higher rate of change, in other words a higher bandwidth or more responsive vehicle, can tolerate smaller values of the distance *d* and still be stable.

C. STABILITIY OF THREE VESSELS

The controller gains for the first vessel are from Equation (25)

$$k_{11} = \frac{-\omega_{n_1}{}^2}{b_1}$$
$$k_{21} = \frac{-(a_1 + 2\zeta_1\omega_{n_1})}{b_1} \qquad (48)$$

for the second vessel

$$k_{12} = \frac{-\omega_{n_2}{}^2}{b_2}$$
$$k_{22} = \frac{-(a_2 + 2\zeta_2\omega_{n_2})}{b_2} \qquad (49)$$

and for the third vessel

$$k_{23} = \frac{-\omega_{n_3}{}^2}{b_3}$$
$$k_{33} = \frac{-(a_3 + 2\zeta_3\omega_{n_3})}{b_3} \qquad (50)$$

This time the linearized system matrix A in Equation (36) turns out to be a 9 by 9 matrix.

$$A = \begin{bmatrix} 0 & 1 & 0 & 0 & 0 & 0 & 0 & 0 & 0 \\ -\omega_{n_1}{}^2 & -2\zeta_1\omega_{n_1} & \frac{-\omega_{n_1}{}^2}{d_1} & 0 & 0 & 0 & 0 & 0 & 0 \\ 1 & 0 & 0 & 0 & 0 & 0 & 0 & 0 & 0 \\ 0 & 0 & 0 & 0 & 1 & 0 & 0 & 0 & 0 \\ 0 & 0 & \frac{\omega_{n_2}{}^2}{d_2} & -\omega_{n_2}{}^2 & -2\zeta_2\omega_{n_2} & \frac{-\omega_{n_2}{}^2}{d_2} & 0 & 0 & 0 \\ 0 & 0 & 0 & 1 & 0 & 0 & 0 & 0 & 0 \\ 0 & 0 & 0 & 0 & 0 & 0 & 0 & 1 & 0 \\ 0 & 0 & 0 & 0 & 0 & \frac{\omega_{n_3}{}^2}{d_3} & -\omega_{n_3}{}^2 & -2\zeta_3\omega_{n_3} & \frac{-\omega_{n_3}{}^2}{d_3} \\ 0 & 0 & 0 & 0 & 0 & 0 & 1 & 0 & 0 \end{bmatrix} \qquad (51)$$

The study of the eigenvalues of matrix A can reveal the local stability properties of the string. First, we develop the characteristic equation of matrix A

$$\lambda^9+(\frac{\lambda^8}{d_1d_2d_3}(2\zeta_1\omega_{n_1}+2\zeta_2\omega_{n_2}+2\zeta_3\omega_{n_3}))+(\frac{\lambda^7}{d_1d_2d_3}(\omega_{n_1}{}^2+4\zeta_1\zeta_2\omega_{n_1}\omega_{n_2}+4\zeta_1\zeta_3\omega_{n_1}\omega_{n_3}+\omega_{n_2}{}^2+$$
$$4\zeta_2\zeta_3\omega_{n_2}\omega_{n_3}+\omega_{n_3}{}^2))+(\frac{\lambda^6}{d_1d_2d_3}(2\zeta_2\omega_{n_1}{}^2\omega_{n_2}+2\zeta_3\omega_{n_1}{}^2\omega_{n_3}+\frac{\omega_{n_1}{}^2}{d_1}+2\zeta_1\omega_{n_1}\ \omega_{n_2}{}^2+8\zeta_1\zeta_2\zeta_3\omega_{n_1}\omega_{n_2}\omega_{n_3}+$$
$$2\zeta_1\omega_{n_1}\ \omega_{n_3}{}^2+2\zeta_3\omega_{n_2}{}^2\omega_{n_3}+\frac{\omega_{n_2}{}^2}{d_2}+2\zeta_2\omega_{n_2}\ \omega_{n_3}{}^2+\frac{\omega_{n_3}{}^2}{d_3}))+(\frac{\lambda^5}{d_1d_2d_3}(\omega_{n_1}{}^2\omega_{n_2}{}^2+4\zeta_2\zeta_3\omega_{n_1}{}^2\omega_{n_2}\omega_{n_3}+$$
$$\frac{2\zeta_2\omega_{n_1}{}^2\omega_{n_2}}{d_1}+\omega_{n_1}{}^2\omega_{n_3}{}^2+\frac{2\zeta_3\omega_{n_1}{}^2\omega_{n_3}}{d_1}+4\zeta_1\zeta_3\omega_{n_1}\omega_{n_2}{}^2\omega_{n_3}+\frac{2\zeta_1\omega_{n_1}\omega_{n_2}{}^2}{d_2}+4\zeta_1\zeta_2\omega_{n_1}\omega_{n_2}\omega_{n_3}{}^2+\frac{2\zeta_1\omega_{n_1}\omega_{n_3}{}^2}{d_3}+$$
$$\omega_{n_2}{}^2\omega_{n_3}{}^2+\frac{2\zeta_3\omega_{n_2}{}^2\omega_{n_3}}{d_2}+\frac{2\zeta_2\omega_{n_2}\omega_{n_3}{}^2}{d_3}))+(\frac{\lambda^4}{d_1d_2d_3}(\frac{\omega_{n_1}{}^2\omega_{n_3}{}^2}{d_3}+\frac{\omega_{n_1}{}^2\omega_{n_2}{}^2}{d_2}+\frac{\omega_{n_2}{}^2\omega_{n_3}{}^2}{d_3}+\frac{\omega_{n_1}{}^2\omega_{n_2}{}^2}{d_1}+\frac{\omega_{n_2}{}^2\omega_{n_3}{}^2}{d_2}+$$
$$\frac{\omega_{n_1}{}^2\omega_{n_3}{}^2}{d_1}+2\zeta_1\omega_{n_1}\omega_{n_2}{}^2\omega_{n_3}{}^2+2\zeta_2\omega_{n_1}{}^2\omega_{n_2}\omega_{n_3}{}^2+2\zeta_3\omega_{n_1}{}^2\omega_{n_2}{}^2\omega_{n_3}+\frac{4\zeta_1\zeta_2\omega_{n_1}\omega_{n_2}\omega_{n_3}{}^2}{d_3}+\frac{4\zeta_1\zeta_3\omega_{n_1}\omega_{n_2}{}^2\omega_{n_3}}{d_2}+$$
$$\frac{4\zeta_2\zeta_3\omega_{n_1}{}^2\omega_{n_2}\omega_{n_3}}{d_1}))+(\frac{\lambda^3}{d_1d_2d_3}(\frac{\omega_{n_2}{}^2\omega_{n_3}{}^2}{d_2d_3}+\frac{\omega_{n_1}{}^2\omega_{n_3}{}^2}{d_1d_3}+\frac{\omega_{n_1}{}^2\omega_{n_2}{}^2}{d_1d_2}+\omega_{n_1}{}^2\omega_{n_2}{}^2\omega_{n_3}{}^2+\frac{2\zeta_1\omega_{n_1}\omega_{n_2}{}^2\omega_{n_3}{}^2}{d_3}+$$
$$\frac{2\zeta_2\omega_{n_1}{}^2\omega_{n_2}\omega_{n_3}{}^2}{d_3}+\frac{2\zeta_1\omega_{n_1}\omega_{n_2}{}^2\omega_{n_3}{}^2}{d_2}+\frac{2\zeta_3\omega_{n_1}{}^2\omega_{n_2}{}^2\omega_{n_3}}{d_2}+\frac{2\zeta_2\omega_{n_1}{}^2\omega_{n_2}\omega_{n_3}{}^2}{d_1}+\frac{2\zeta_3\omega_{n_1}{}^2\omega_{n_2}{}^2\omega_{n_3}}{d_1}))+(\frac{\lambda^2}{d_1d_2d_3}$$
$$(\frac{2\zeta_1\omega_{n_1}\omega_{n_2}{}^2\omega_{n_3}{}^2}{d_2d_3}+\frac{2\zeta_2\omega_{n_1}{}^2\omega_{n_2}\omega_{n_3}{}^2}{d_1d_3}+\frac{2\zeta_3\omega_{n_1}{}^2\omega_{n_2}{}^2\omega_{n_3}}{d_1d_2}+\frac{\omega_{n_1}{}^2\omega_{n_2}{}^2\omega_{n_3}{}^2}{d_3}+\frac{\omega_{n_1}{}^2\omega_{n_2}{}^2\omega_{n_3}{}^2}{d_2}+\frac{\omega_{n_1}{}^2\omega_{n_2}{}^2\omega_{n_3}{}^2}{d_1}))+$$
$$(\frac{\lambda}{d_1d_2d_3}(\frac{\omega_{n_1}{}^2\omega_{n_2}{}^2\omega_{n_3}{}^2}{d_2d_3}+\frac{\omega_{n_1}{}^2\omega_{n_2}{}^2\omega_{n_3}{}^2}{d_1d_3}+\frac{\omega_{n_1}{}^2\omega_{n_2}{}^2\omega_{n_3}{}^2}{d_1d_2}))+\frac{\omega_{n_1}{}^2\omega_{n_2}{}^2\omega_{n_3}{}^2}{d_1d_2d_3}=0 \quad (52)$$

Following some algebra, we can show that this is the product of the following three equations

$$\lambda^3+2\zeta_1\omega_{n_1}\lambda^2+\omega_{n_1}{}^2\lambda+\frac{\omega_{n_1}{}^2}{d_1}=0 \quad \lambda^3+2\zeta_2\omega_{n_2}\lambda^2+\omega_{n_2}{}^2\lambda+\frac{\omega_{n_2}{}^2}{d_2}=0 \quad \text{and}$$
$$\lambda^3+2\zeta_3\omega_{n_3}\lambda^2+\omega_{n_3}{}^2\lambda+\frac{\omega_{n_3}{}^2}{d_3}=0 \quad (53)$$

Equation (53) is essentially the same form as Equation (43), which is the characteristic equation for the case of one vessel trying to move in the commanded path.

The characteristic equation of matrix A then becomes

$$(\lambda^3+2\zeta_1\omega_{n_1}\lambda^2+\omega_{n_1}{}^2\lambda+\frac{\omega_{n_1}{}^2}{d_1})\cdot(\lambda^3+2\zeta_2\omega_{n_2}\lambda^2+\omega_{n_2}{}^2\lambda+\frac{\omega_{n_2}{}^2}{d_2})\cdot(\lambda^3+2\zeta_3\omega_{n_3}\lambda^2+\omega_{n_3}{}^2\lambda+\frac{\omega_{n_3}{}^2}{d_3})=0 \quad (54)$$

Therefore, the nine eigenvalues of matrix A are the roots of Equation (53). In other words, the eigenvalues for the case of three vessels independently try to follow the commanded path. This means that system stability is established if and only if all the

vessels have stability under the assumption that they move independently (not in a string, but separately), as in

$$d_1 > \frac{1}{2\zeta_1\omega_{n_1}} \quad , \quad d_2 > \frac{1}{2\zeta_2\omega_{n_2}} \quad \text{and} \quad d_3 > \frac{1}{2\zeta_3\omega_{n_3}} \tag{55}$$

THIS PAGE INTENTIONALLY LEFT BLANK

IV. PARAMETRIC STUDIES

A. INTRODUCTION

In this chapter, parametric studies of marine surface vehicle stability conditions are introduced. A maneuvering prediction program was used to evaluate the hydrodynamic coefficients for a range of vehicle geometric parameters. Using this program, the coefficients in Nomoto's model was evaluated. Then, we looked at the variation of the critical parameter for stability in terms of vehicle geometry.

B. MANEUVERING PREDICTION PROGRAM

The Maneuvering Prediction Program (MPP) we utilized here was first developed to support the teaching of conceptual ship design within the University of Michigan's Department of Naval Architecture and Marine Engineering. This program applies methods to assess the course stability, turn ability, and controllability of a surface marine vehicle. While applying these methods, the MPP uses the following empirical equations in Equation (56)

$$
\begin{aligned}
Y_{\dot{v}} &= -\pi(\frac{T}{L})^2\left[1+0.16C_B\frac{B}{T}-5.1(\frac{B}{L})^2\right],\\
Y_{\dot{r}} &= -\pi(\frac{T}{L})^2\left[0.67\frac{B}{L}-0.0033(\frac{B}{T})^2\right],\\
N_{\dot{v}} &= -\pi(\frac{T}{L})^2\left[1.1\frac{B}{L}-0.041\frac{B}{T}\right],\\
N_{\dot{r}} &= -\pi(\frac{T}{L})^2\left[\frac{1}{12}+0.017C_B\frac{B}{T}-0.33\frac{B}{L}\right],\\
Y_{v} &= -\pi(\frac{T}{L})^2\left[1+0.40C_B\frac{B}{T}\right],\\
Y_{r} &= -\pi(\frac{T}{L})^2\left[-\frac{1}{2}+2.2\frac{B}{L}-0.080\frac{B}{T}\right],\\
N_{v} &= -\pi(\frac{T}{L})^2\left[\frac{1}{2}+2.4\frac{T}{L}\right],\\
N_{r} &= -\pi(\frac{T}{L})^2\left[\frac{1}{4}+0.039\frac{B}{T}-0.56\frac{B}{L}\right]
\end{aligned}
\qquad (56)
$$

where B, T, L are the maximum beam, the mean draft and the length on waterline, respectively. $Y_{\dot{v}}, Y_{\dot{r}}, N_{\dot{v}}, N_{\dot{r}}, Y_v, Y_r, N_v, N_r$ are the vessel hydrodynamic derivatives. These formulas form the basis of the predictions incorporated in the MPP, although additional, primarily empirical, adjustments based on [3] and [4], are made in the program.

The vehicle characteristics input to the MPP are listed in Table 1.

Vehicle Characteristics		
Length on Waterline (LWL)	100	Meters
Maximum Beam (B)	10	Meters
Draft Forward (TF)	7	Meters
Draft Aft (TA)	7	Meters
Block Coefficient on LWL (CB)	0.7	-

Table 1. Vessel characteristics used in MPP.

Parametric studies were performed in three separate parts. Beam, block coefficient and mean draft effects on critical distances are analyzed. Typical outputs from the MPP for each effect are included in the appendix.

C. BEAM EFFECTS

In order to present the beam effects on the critical stability distance, we kept the beam of the model as a variable, and the remaining vehicle characteristics are set to be constant as shown in Table 1. Using the MPP and the previous parametric expressions, we calculated the T and K maneuverability indexes for each value of different beam values assuming that the surface vehicle was hydrodynamically course stable. Results for hydrodynamically course unstable vehicles were discarded as they were believed to be unreliable and could not be adequately modeled by the MPP's parametric formulas. Typical results for different beam values are listed in Table 2.

Maximum Beam on Waterline (B) (meters)	Time Constant (T)	Rudder Gain Factor (K)
7	0.8427	-0.5704
8	1.0534	-0.6677
9	1.3215	-0.7935
10	1.6706	-0.96
11	2.1398	-1.1875
12	2.798	-1.5117
13	3.7808	-2.0028
14	5.3941	-2.8191
15	8.5058	-4.4104
16	16.9337	-8.7544

Table 2. Calculated values of T and K maneuverability ındexes for different beam values.

We already referred to Nomoto's first order model in Equation (20) and expressed it in the form in Equation (21). Now we can calculate the new maneuverability indexes, a and b, which have already been defined in Equation (21). These a and b values for different beam values are listed in Table 3.

Maximum Beam on Waterline (B) (meters)	a (-1/T)	b (K/T)
7	-1.1867	-0.6769
8	-0.9493	-0.6339
9	-0.7567	-0.6004
10	-0.5986	-0.5746
11	-0.4673	-0.5549
12	-0.3574	-0.5403
13	-0.2645	-0.5297
14	-0.1854	-0.5226
15	-0.1176	-0.5185
16	-0.0590	-0.5170

Table 3. Calculated values of new maneuverability indexes for different beam values.

Knowing the a and b values allows us to calculate ω_n and ζ by using Equation (45) and Equation (46). The calculations were made by using the following values for the parameters:

1. Controller gain k_1: $k_1 = 2$

2. Controller gain k_2: $k_2 = -2.5$

Calculated ω_n and ζ values for different beam values are listed in Table 4.

Maximum Beam on Waterline (B) (meters)	ω_n	ζ
7	1.1635	0.2172
8	1.1259	0.2821
9	1.0958	0.3396
10	1.0720	0.3908
11	1.0535	0.4366
12	1.0395	0.4778
13	1.0293	0.5148
14	1.0224	0.5483
15	1.0183	0.5787
16	1.0168	0.6065

Table 4. Calculated ω_n and ζ values for different beam values.

Now either Equation (44) or Equation (47) can be used to determine the $d_{critical}$ values. The results of $d_{critical}$ values for different beam values are listed in Table 5.

Maximum Beam on Waterline (B) (meters)	$d_{critical}$
7	1.9782
8	1.5740
9	1.3433
10	1.1933
11	1.0869
12	1.0067
13	0.9435
14	0.8919
15	0.8483
16	0.8107

Table 5. Calculated $d_{critical}$ values for different beam values.

The values in Table 5 were used to plot the beam effects on $d_{critical}$ values. Figure 4 presents $d_{critical}$ values for different beam values. Analyzing Figure 4 brings us to our main conclusion about beam effects. We conclude that the critical distance is decreasing for the increasing beam; therefore, wider vehicles can maintain string formation stability more easily.

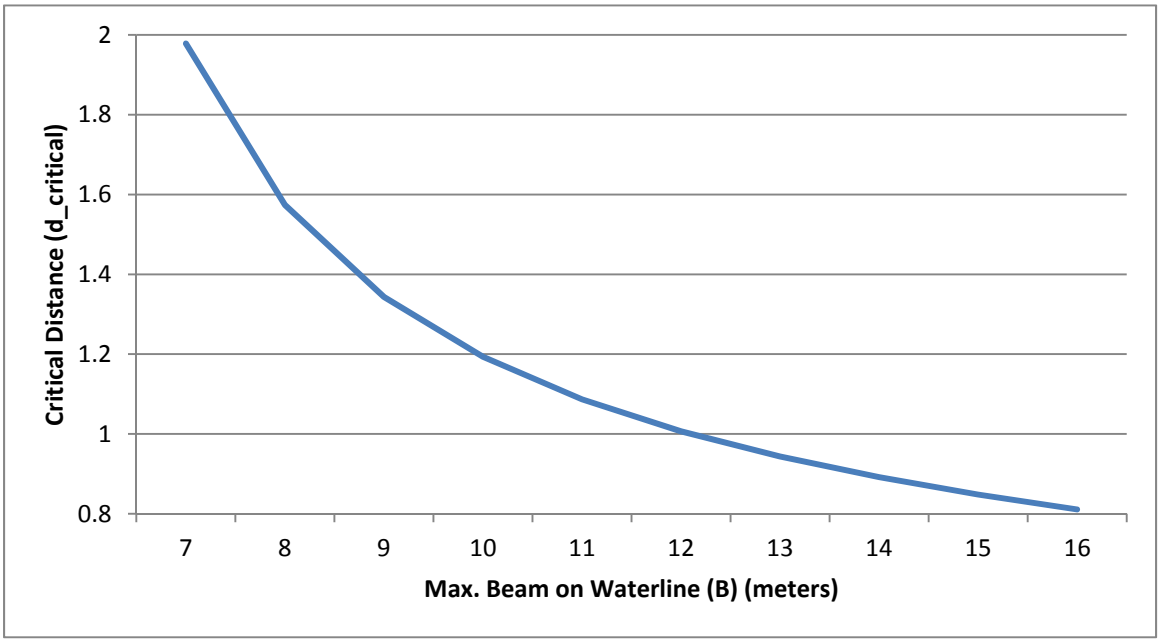

Figure 4. Beam effects on critical distance values.

D. BLOCK COEFFICIENT EFFECTS

Block coefficient is the ratio of the volume of displacement at any draft to the volume of a rectangular block with dimensions equal to the ship length, the ship beam and the draft. In order to analyze the block coefficient effects on critical distance, a similar method used for beam effect calculations is applied. This time the block coefficient values are set as the independent variable and the remaining vehicle characteristics are set to be constant as in Table 1. Using MPP, the T and K maneuverability indexes are calculated for each value of different block coefficient values for which marine surface vehicle is hydrodynamically course stable. The results for different C_B values are listed in Table 6.

Block Coefficient (C_B)	Time Constant (T)	Rudder Gain Factor (K)
0.52	0.9087	-0.6973
0.56	1.0403	-0.7438
0.6	1.1902	-0.7961
0.64	1.3619	-0.8553
0.68	1.56	-0.9226
0.72	1.7902	-1.0001
0.76	2.0605	-1.0902
0.8	2.3814	-1.1962
0.84	2.7675	-1.3227
0.88	3.2397	-1.4764

Table 6. Calculated values of T and K maneuverability ındexes for different block coefficient values.

As previously done in Beam Effects calculations, the new maneuverability indexes, a and b, can be calculated. Calculated a and b values for different block coefficient values are listed in Table 7.

Block Coefficient (C_B)	a (-1/T)	b (K/T)
0.52	-1.1005	-0.7673
0.56	-0.9613	-0.7150
0.6	-0.8402	-0.6689
0.64	-0.7343	-0.6280
0.68	-0.6410	-0.5914
0.72	-0.5586	-0.5586
0.76	-0.4853	-0.5291
0.8	-0.4199	-0.5023
0.84	-0.3613	-0.4779
0.88	-0.3087	-0.4557

Table 7. Calculated values of new maneuverability indexes for different block coefficient values.

Similarly, ω_n and ζ can be calculated by using Equation (45) and Equation (46). For consistency, the same controller gain values were used. Calculated ω_n and ζ values for different block coefficient values are listed in Table 8.

Block Coefficient (C_B)	ω_n	ζ
0.52	1.2388	0.3301
0.56	1.1958	0.3454
0.6	1.1566	0.3597
0.64	1.1207	0.3729
0.68	1.0876	0.3850
0.72	1.0570	0.3964
0.76	1.0287	0.4070
0.8	1.0023	0.4169
0.84	0.9777	0.4263
0.88	0.9547	0.4350

Table 8. Calculated ω_n and ζ values for different block coefficient values.

The results of $d_{critical}$ values for different block coefficient values are listed in Table 9.

Block Coefficient (C_B)	$d_{critical}$
0.52	1.2226
0.56	1.2104
0.6	1.2019
0.64	1.1965
0.68	1.1940
0.72	1.1933
0.76	1.1941
0.8	1.1964
0.84	1.1997
0.88	1.2039

Table 9. Calculated $d_{critical}$ values for different block coefficient values.

Figure 5 shows the block coefficient effect on critical distance. It can be seen from Figure 5 that there is an optimum block coefficient for formation stability properties.

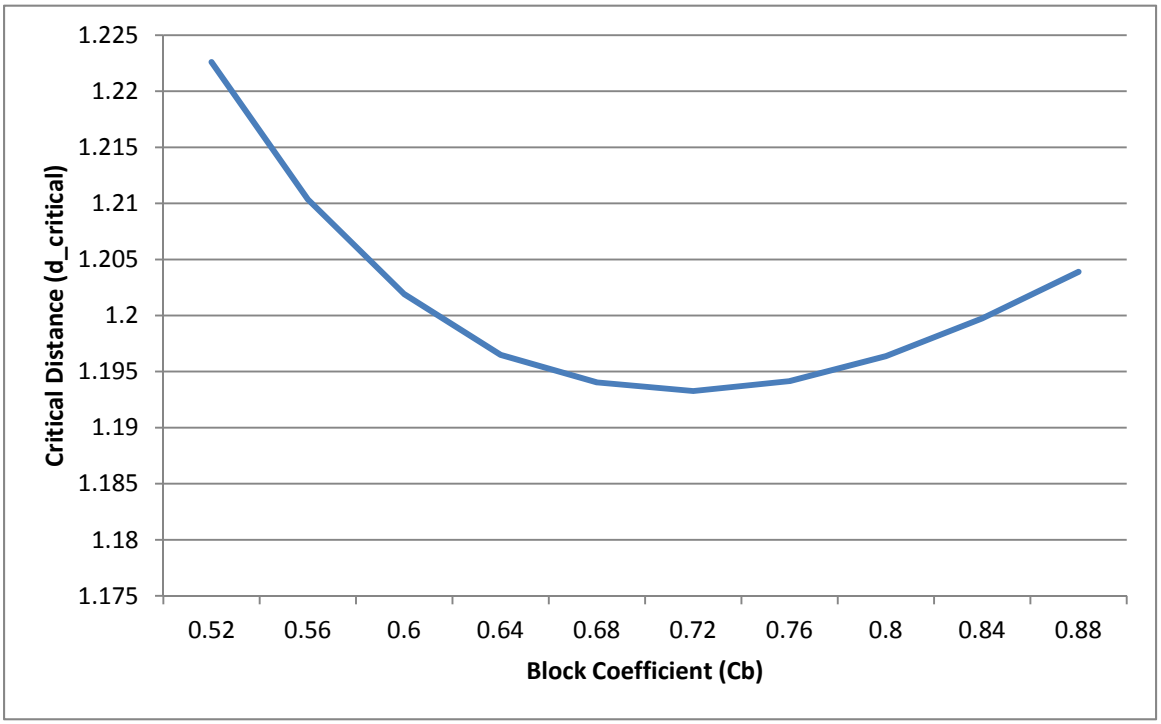

Figure 5. Block coefficient effects on critical distance values.

E. MEAN DRAFT EFFECTS

In this section, the same method is used to determine the maneuverability indexes (T, K, a and b), ω_n, ζ and $d_{critical}$ values. The procedure to calculate these variables has already been explained in the previous sections.

The results of maneuverability indexes T and K for different mean draft values are listed in Table 10.

Mean Draft (meters)	Time Constant (T)	Rudder Gain Factor (K)
1	3.1479	-1.7052
2	4.4297	-2.3283
3	4.1638	-2.2236
4	3.3379	-1.8206
5	2.6011	-1.4468
6	2.0588	-1.1651
7	1.6706	-0.96
8	1.3885	-0.809
9	1.178	-0.6952
10	1.0166	-0.6073
11	0.8896	-0.5379

Table 10. Calculated values of T and K maneuverability ındexes for different mean draft values.

Calculated a and b values for different mean draft values are listed in Table 11.

Mean Draft (meters)	a (-1/T)	b (K/T)
1	-0.3177	-0.5417
2	-0.2257	-0.5256
3	-0.2402	-0.5340
4	-0.2996	-0.5454
5	-0.3844	-0.5562
6	-0.4857	-0.5659
7	-0.5986	-0.5746
8	-0.7202	-0.5826
9	-0.8489	-0.5901
10	-0.9837	-0.5974
11	-1.1241	-0.6046

Table 11. Calculated values of new maneuverability indexes for different mean draft values.

Calculated ω_n and ζ values for different mean draft values are listed in Table 12.

Mean Draft (meters)	ω_n	ζ
1	1.0408	0.4979
2	1.0253	0.5307
3	1.0335	0.5297
4	1.0444	0.5093
5	1.0547	0.4769
6	1.0639	0.4366
7	1.0720	0.3908
8	1.0795	0.3411
9	1.0864	0.2883
10	1.0930	0.2332
11	1.0997	0.1762

Table 12. Calculated ω_n and ζ values for different mean draft values.

The results of $d_{critical}$ values for different mean draft values are listed in Table 13.

Mean Draft (meters)	$d_{critical}$
1	0.9647
2	0.9189
3	0.9133
4	0.9398
5	0.9939
6	1.0763
7	1.1933
8	1.3579
9	1.5962
10	1.9616
11	2.5804

Table 13. Calculated $d_{critical}$ values for different mean draft values.

Figure 6 represents the block coefficient effects on critical distance. Focusing on Figure 6, we can say that a shallow draft is preferable although an optimum may exist for formation stability properties.

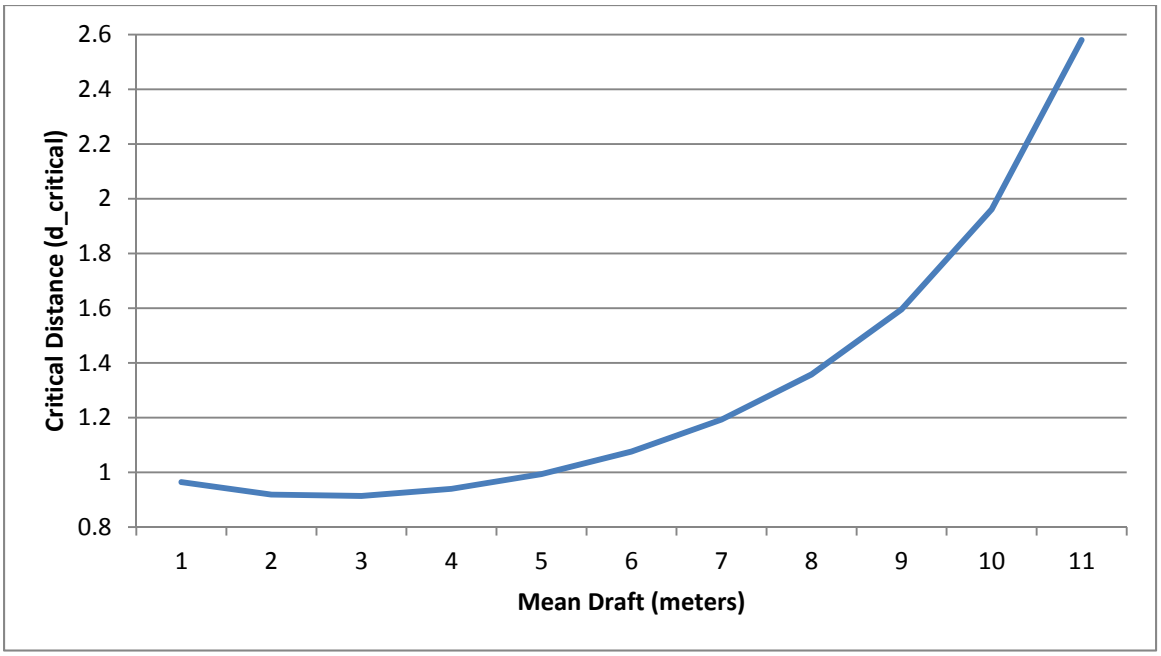

Figure 6. Mean draft effects on critical distance values.

V. CONCLUSIONS AND RECOMMENDATIONS

A. CONCLUSIONS

This thesis addressed the problem of coordinated motion control and the stability loss of surface marine vehicles. The problem was decoupled into the motion stability control task of making each marine surface vehicle follow a target along its path.

The main work and results are summarized as follows:

1. A mathematical model was derived which is based on Nomoto's second order model and captures the fundamental dynamics of turning on the horizontal plane with no side slip.
2. A state feedback control law was coupled with a line of sight guidance law to provide path control. A string of three vehicles was considered where each vehicle is using the vehicle in the front as a reference point.
3. The coupled motion stability of the formation was analyzed by linearization. It was shown that under the assumed dynamics, guidance, and control laws, the stability properties of the system decouple into individual vehicles. This makes it possible to obtain exact analytical results that can be used in design.
4. Parametric runs and sensitivity analysis studies revealed the effects of main vehicle geometric parameters on formation control and motion stability.
5. It was established that the critical stability coefficient is a function of the derivative gain of the control law.
6. The critical stability coefficient depends as follows on vehicle geometry:
    a. It is decreasing for increasing vehicle beam.
    b. It is in general increasing for increasing draft.
    c. It has an optimum in terms of the block coefficient.

B. RECOMMENDATIONS

The study presented in this thesis can be extended in different areas, briefly explained below.

The main recommendations for future research are summarized as follows:

1. Analyze the nonlinear behavior of the system in order to see if there are higher order effects that could not be captured by linearization.
2. Expand the range of parametric studies to additional variables such as forward speed and develop a set of design recommendations.
3. Finally, incorporate the longitudinal equations of motion by allowing the distances d_1, d_2, and d_3 to be functions of time.

APPENDIX

Project Name: Beam Effects Sat Jun 08 13:47:40 2013

University of Michigan
Department of Naval Architecture and Marine Engineering

Maneuvering Prediction Program (MPP-1.3) by M.G. Parsons

References: Clarke,D., Gedling,P., and Hine,G.,
"The Application of Manoeuvring Criteria in Hull Design using Linear Theory," Trans. RINA, 1983
Lyster, C., and Knights, H. L.,
"Prediction Equations for Ships' Turning Circles," Trans. NECIES, 1978-1979

Run Identification: Beam Effects

Input Verification:

Length of Waterline LWL (m)	=	100.00
Maximum Beam on LWL (m)	=	12.00
Mean Draft (m)	=	7.00
Draft Forward (m)	=	7.00
Draft Aft (m)	=	7.00
Block Coefficient on LWL CB	=	0.7000
Molded Volume (m^3)	=	5880.00
Center of Gravity LCG (%LWL; + Fwd)	=	0.0000
Center of Gravity LCG (m from FP)	=	50.00
Midships to Rudder CE XR (%LWL; + Aft)	=	49.0000
Rudder Center of Effort XR (m from FP)	=	99.00
Initial Ship Speed (knots)	=	15.00
Initial Ship Speed (m/s)	=	7.7166
Water Type	=	Salt@15C
Water Density (kg/m^3)	=	1025.87
Kinematic Viscosity (m^2/s)	=	0.118831E-05
Yaw Radius of Gyration K33/LWL	=	0.2500
Water Depth to Ship Draft Ratio H/T	=	1000.00
Steering Gear Time Constant (s)	=	2.50
Total Rudder Area - Fraction of LWL*T	=	0.0136
Number of Propellers	=	1
Type of Single Screw Stern	=	Closed
Submerged Bow Area - Fraction of LWL*T	=	0.0000

1

University of Michigan
Department of Naval Architecture and Marine Engineering

Maneuvering Prediction Program (MPP-1.3) by M.G. Parsons

*** Linear Maneuvering Criteria Option ***

Reference: Clarke,D., Gedling,P., and Hine,G.,
"The Application of Manoeuvring Criteria in Hull
Design using Linear Theory," Trans. RINA, 1983

Run Identification: Beam Effects

Linear Maneuvering Derivatives

Nondimensional Mass	M prime	= 0.011760
Nondimensional Mass Moment	I sub zz	= 0.000735
Sway Velocity Derivative	Y sub v	= -0.023640
Sway Acceleration Derivative	Y sub v dot	= -0.017219
Yaw Velocity Derivative	N sub v	= -0.009863
Yaw Acceleration Derivative	N sub v dot	= -0.000950
Sway Velocity Derivative	Y sub r	= 0.006164
Sway Acceleration Derivative	Y sub r dot	= -0.001088
Yaw Velocity Derivative	N sub r	= -0.004049
Yaw Acceleration Derivative	N sub r dot	= -0.000987
Sway Rudder Derivative	Y sub delta	= 0.002856
Yaw Rudder Derivative	N sub delta	= -0.001399

Time Constants and Gains for Nomoto"s Equation

Dominant Ship Time Constant	T1 prime	= 3.1175
Ship Time Constant	T2 prime	= 0.3869
Numerator Time Constant	T3 prime	= 0.7064
Numerator Time Constant	T4 prime	= 0.3321
1st Order Eqn. Time Constant	T prime	= 2.7980
Rudder Gain Factor	K prime	= -1.5117
Rudder Gain Factor	K sub v prime	= 0.4787
Steering Gear Time Constant	TE prime	= 0.1929

Evaluation of Turning Ability and Stability

Inverse Time Constant	1/|T prime|	= 0.3574
Inverse Gain Factor	1/|K prime|	= 0.6615
Clarke"s Turning Index	P	= 0.3065
Linear Dynamic Stability Criterion	C	= 0.0000405

Vessel is hydrodynamically open loop course stable

Closed Loop Phase Margin with Steering Engine = 28.5803 degrees

University of Michigan
Department of Naval Architecture and Marine Engineering

Maneuvering Prediction Program (MPP-1.3) by M.G. Parsons

*** Turning Prediction Option ***

Reference: Lyster, C., and Knights, H. L.,
"Prediction Equations for Ships' Turning Circle",
Trans. NECIES, 1978-1979

Run Identification: Beam Effects

Approach Speed	-	15.00 knots
Rudder Angle	-	10.00 degrees
Steady Turning Diameter	-	758.41 meters
Tactical Diameter	-	791.10 meters
Advance	-	540.97 meters
Transfer	-	386.80 meters
Steady Speed in Turn	-	11.19 knots

```
Project Name: Beam Effects                          Sat Jun 08 13:47:40 2013

                    University of Michigan
 Department of Naval Architecture and Marine Engineering

Maneuvering Prediction Program (MPP-1.3) by M.G. Parsons

 ***State Variable Equations Option ***

 Run Identification: Beam Effects

     [psi]    [ 0  1   0  ][psi]    [0 ]
 d/dt[ r ] = [ 0 a22 a23 ][ r ] + [b2] delta
     [ v ]    [ 0 a32 a33 ][ v ]    [b3]

                [    0          0   ]
              + [gamma 21  gamma 22][Y external]
                [gamma 31  gamma 32][N external]

 Open Loop Dynamics Matrix Coeff.          a22 =    -2.29188
 Open Loop Dynamics Matrix Coeff.          a23 =     5.38858
 Open Loop Dynamics Matrix Coeff.          a32 =     0.17521
 Open Loop Dynamics Matrix Coeff.          a33 =    -0.61337

 Control Distribution Matrix Coeff.         b2 =    -0.88527
 Control Distribution Matrix Coeff.         b3 =    -0.13180

 Ext. Force Distr. Matrix Coeff.     gamma 21 =   -19.43766
 Ext. Force Distr. Matrix Coeff.     gamma 22 =   592.91730
 Ext. Force Distr. Matrix Coeff.     gamma 31 =   -35.23790
 Ext. Force Distr. Matrix Coeff.     gamma 32 =    22.26846

                                     4
```

Figure 7. One of the outputs of the MPP for beam effects.

University of Michigan
Department of Naval Architecture and Marine Engineering

Maneuvering Prediction Program (MPP-1.3) by M.G. Parsons

References: Clarke,D., Gedling,P., and Hine,G.,
"The Application of Manoeuvring Criteria in Hull Design using Linear Theory," Trans. RINA, 1983
Lyster, C., and Knights, H. L.,
"Prediction Equations for Ships' Turning Circles," Trans. NECIES, 1978-1979

Run Identification: Block Coefficient Effects

Input Verification:

Length of Waterline LWL (m)	=	100.00
Maximum Beam on LWL (m)	=	10.00
Mean Draft (m)	=	7.00
Draft Forward (m)	=	7.00
Draft Aft (m)	=	7.00
Block Coefficient on LWL CB	=	0.8000
Molded Volume (m^3)	=	5600.00
Center of Gravity LCG (%LWL; + Fwd)	=	0.0000
Center of Gravity LCG (m from FP)	=	50.00
Midships to Rudder CE XR (%LWL; + Aft)	=	49.0000
Rudder Center of Effort XR (m from FP)	=	99.00
Initial Ship Speed (knots)	=	15.00
Initial Ship Speed (m/s)	=	7.7166
Water Type	=	Salt@15C
Water Density (kg/m^3)	=	1025.87
Kinematic Viscosity (m^2/s)	=	0.118831E-05
Yaw Radius of Gyration K33/LWL	=	0.2500
Water Depth to Ship Draft Ratio H/T	=	1000.00
Steering Gear Time Constant (s)	=	2.50
Total Rudder Area - Fraction of LWL*T	=	0.0125
Number of Propellers	=	1
Type of Single Screw Stern	=	Closed
Submerged Bow Area - Fraction of LWL*T	=	0.0000

University of Michigan
Department of Naval Architecture and Marine Engineering

Maneuvering Prediction Program (MPP-1.3) by M.G. Parsons

*** Linear Maneuvering Criteria Option ***

Reference: Clarke,D., Gedling,P., and Hine,G.,
"The Application of Manoeuvring Criteria in Hull
Design using Linear Theory," Trans. RINA, 1983

Run Identification: Block Coefficient Effects

Linear Maneuvering Derivatives

Nondimensional Mass	M prime	= 0.011200
Nondimensional Mass Moment	I sub zz	= 0.000700
Sway Velocity Derivative	Y sub v	= -0.023218
Sway Acceleration Derivative	Y sub v dot	= -0.017424
Yaw Velocity Derivative	N sub v	= -0.009897
Yaw Acceleration Derivative	N sub v dot	= -0.000792
Sway Velocity Derivative	Y sub r	= 0.006455
Sway Acceleration Derivative	Y sub r dot	= -0.000928
Yaw Velocity Derivative	N sub r	= -0.004033
Yaw Acceleration Derivative	N sub r dot	= -0.001074
Sway Rudder Derivative	Y sub delta	= 0.002625
Yaw Rudder Derivative	N sub delta	= -0.001286

Time Constants and Gains for Nomoto"s Equation

Dominant Ship Time Constant	T1 prime	= 2.6776
Ship Time Constant	T2 prime	= 0.4003
Numerator Time Constant	T3 prime	= 0.6965
Numerator Time Constant	T4 prime	= 0.3505
1st Order Eqn. Time Constant	T prime	= 2.3814
Rudder Gain Factor	K prime	= -1.1962
Rudder Gain Factor	K sub v prime	= 0.3575
Steering Gear Time Constant	TE prime	= 0.1929

Evaluation of Turning Ability and Stability

Inverse Time Constant	1/|T prime|	= 0.4199
Inverse Gain Factor	1/|K prime|	= 0.8360
Clarke"s Turning Index	P	= 0.2706
Linear Dynamic Stability Criterion	C	= 0.0000467

Vessel is hydrodynamically open loop course stable

Closed Loop Phase Margin with Steering Engine = 33.0114 degrees

University of Michigan
Department of Naval Architecture and Marine Engineering

Maneuvering Prediction Program (MPP-1.3) by M.G. Parsons

*** Turning Prediction Option ***

Reference: Lyster, C., and Knights, H. L.,
"Prediction Equations for Ships' Turning Circle",
Trans. NECIES, 1978-1979

Run Identification: Block Coefficient Effects

Approach Speed	-	15.00 knots
Rudder Angle	-	10.00 degrees
Steady Turning Diameter	-	585.81 meters
Tactical Diameter	-	634.03 meters
Advance	-	459.46 meters
Transfer	-	308.74 meters
Steady Speed in Turn	-	9.41 knots

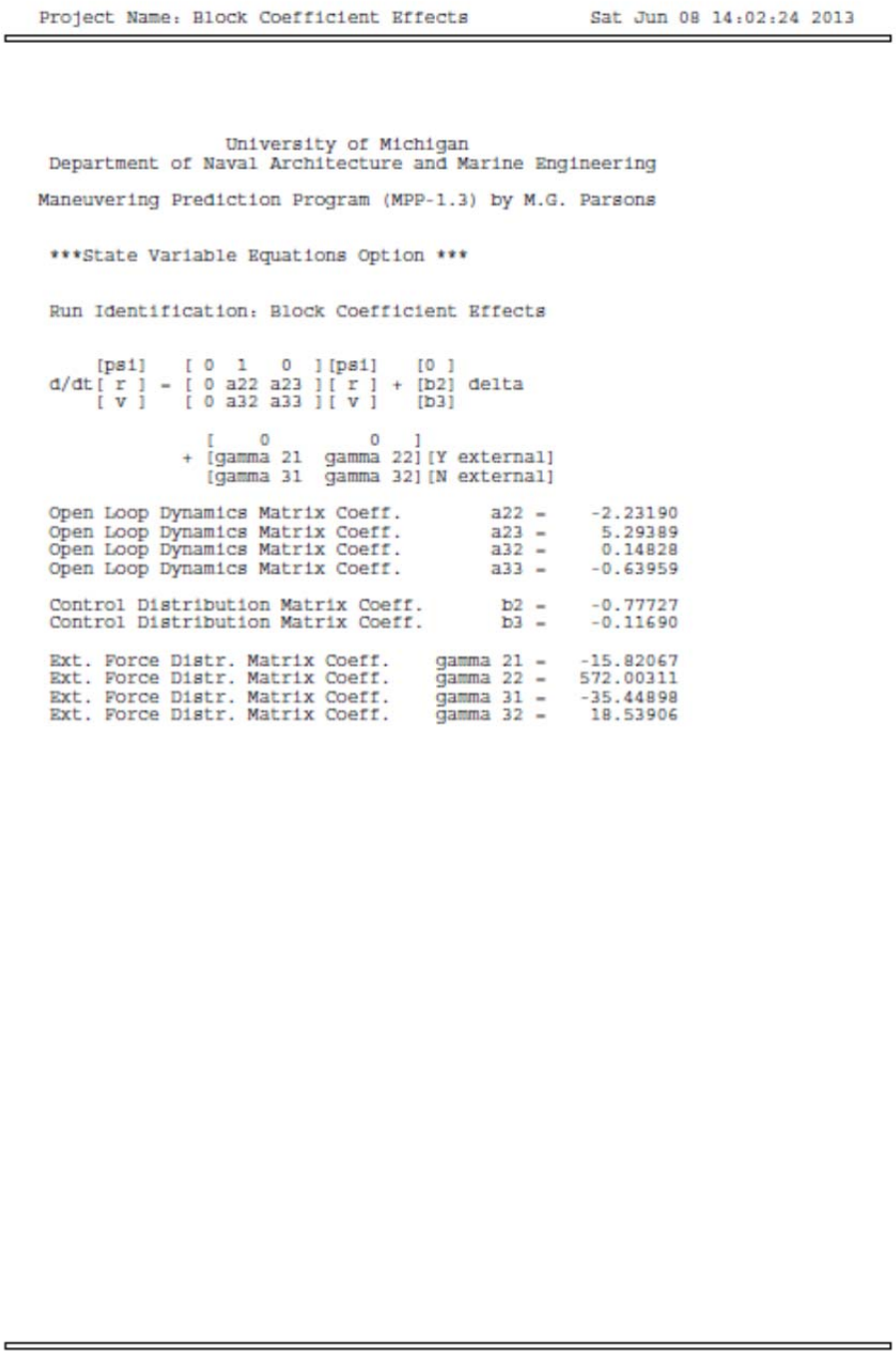

Figure 8. One of the outputs of the MPP for block coefficient effects.

University of Michigan
Department of Naval Architecture and Marine Engineering

Maneuvering Prediction Program (MPP-1.3) by M.G. Parsons

References: Clarke,D., Gedling,P., and Hine,G.,
"The Application of Manoeuvring Criteria in Hull Design using Linear Theory," Trans. RINA, 1983
Lyster, C., and Knights, H. L.,
"Prediction Equations for Ships' Turning Circles," Trans. NECIES, 1978-1979

Run Identification: Mean Draft Effects

Input Verification:

Length of Waterline LWL (m)	=	100.00
Maximum Beam on LWL (m)	=	10.00
Mean Draft (m)	=	5.00
Draft Forward (m)	=	5.00
Draft Aft (m)	=	5.00
Block Coefficient on LWL CB	=	0.7000
Molded Volume (m^3)	=	3500.00
Center of Gravity LCG (%LWL; + Fwd)	=	0.0000
Center of Gravity LCG (m from FP)	=	50.00
Midships to Rudder CE XR (%LWL; + Aft)	=	49.0000
Rudder Center of Effort XR (m from FP)	=	99.00
Initial Ship Speed (knots)	=	15.00
Initial Ship Speed (m/s)	=	7.7166
Water Type	=	Salt@15C
Water Density (kg/m^3)	=	1025.87
Kinematic Viscosity (m^2/s)	=	0.118831E-05
Yaw Radius of Gyration K33/LWL	=	0.2500
Water Depth to Ship Draft Ratio H/T	=	1000.00
Steering Gear Time Constant (s)	=	2.50
Total Rudder Area - Fraction of LWL*T	=	0.0125
Number of Propellers	=	1
Type of Single Screw Stern	=	Closed
Submerged Bow Area - Fraction of LWL*T	=	0.0000

University of Michigan
Department of Naval Architecture and Marine Engineering

Maneuvering Prediction Program (MPP-1.3) by M.G. Parsons

*** Linear Maneuvering Criteria Option ***

Reference: Clarke,D., Gedling,P., and Hine,G.,
"The Application of Manoeuvring Criteria in Hull
Design using Linear Theory," Trans. RINA, 1983

Run Identification: Mean Draft Effects

Linear Maneuvering Derivatives

Nondimensional Mass	M prime	= 0.007000
Nondimensional Mass Moment	I sub zz	= 0.000437
Sway Velocity Derivative	Y sub v	= -0.012815
Sway Acceleration Derivative	Y sub v dot	= -0.009213
Yaw Velocity Derivative	N sub v	= -0.004594
Yaw Acceleration Derivative	N sub v dot	= -0.000220
Sway Velocity Derivative	Y sub r	= 0.003731
Sway Acceleration Derivative	Y sub r dot	= -0.000423
Yaw Velocity Derivative	N sub r	= -0.002271
Yaw Acceleration Derivative	N sub r dot	= -0.000582
Sway Rudder Derivative	Y sub delta	= 0.001875
Yaw Rudder Derivative	N sub delta	= -0.000919

Time Constants and Gains for Nomoto"s Equation

Dominant Ship Time Constant	T1 prime	= 2.9575
Ship Time Constant	T2 prime	= 0.3945
Numerator Time Constant	T3 prime	= 0.7509
Numerator Time Constant	T4 prime	= 0.3168
1st Order Eqn. Time Constant	T prime	= 2.6011
Rudder Gain Factor	K prime	= -1.4468
Rudder Gain Factor	K sub v prime	= 0.5154
Steering Gear Time Constant	TE prime	= 0.1929

Evaluation of Turning Ability and Stability

Inverse Time Constant	1/|T prime|	= 0.3845
Inverse Gain Factor	1/|K prime|	= 0.6912
Clarke"s Turning Index	P	= 0.3168
Linear Dynamic Stability Criterion	C	= 0.0000141

Vessel is hydrodynamically open loop course stable

Closed Loop Phase Margin with Steering Engine = 30.7641 degrees

University of Michigan
Department of Naval Architecture and Marine Engineering

Maneuvering Prediction Program (MPP-1.3) by M.G. Parsons

*** Turning Prediction Option ***

Reference: Lyster, C., and Knights, H. L.,
"Prediction Equations for Ships' Turning Circle",
Trans. NECIES, 1978-1979

Run Identification: Mean Draft Effects

Approach Speed	-	15.00 knots
Rudder Angle	-	10.00 degrees
Steady Turning Diameter	-	784.83 meters
Tactical Diameter	-	815.14 meters
Advance	-	553.45 meters
Transfer	-	398.75 meters
Steady Speed in Turn	-	11.46 knots

```
Project Name: Mean Draft Effects                    Sat Jun 08 14:09:33 2013


                University of Michigan
 Department of Naval Architecture and Marine Engineering

Maneuvering Prediction Program (MPP-1.3) by M.G. Parsons


***State Variable Equations Option ***


Run Identification: Mean Draft Effects


    [psi]    [ 0  1   0  ][psi]    [0 ]
d/dt[ r ] = [ 0 a22 a23 ][ r ] + [b2] delta
    [ v ]    [ 0 a32 a33 ][ v ]    [b3]

             [    0          0   ]
           + [gamma 21  gamma 22][Y external]
             [gamma 31  gamma 32][N external]

Open Loop Dynamics Matrix Coeff.        a22 =    -2.19623
Open Loop Dynamics Matrix Coeff.        a23 =     4.35895
Open Loop Dynamics Matrix Coeff.        a32 =     0.18778
Open Loop Dynamics Matrix Coeff.        a33 =    -0.67681

Control Distribution Matrix Coeff.       b2 =    -0.93114
Control Distribution Matrix Coeff.       b3 =    -0.13992

Ext. Force Distr. Matrix Coeff.    gamma 21 =   -13.37672
Ext. Force Distr. Matrix Coeff.    gamma 22 =   986.18317
Ext. Force Distr. Matrix Coeff.    gamma 31 =   -62.02859
Ext. Force Distr. Matrix Coeff.    gamma 32 =    25.70241


                                4
```

Figure 9. One of the outputs of MPP for mean draft effects.

LIST OF REFERENCES

[1] F. A. Papoulias," On the nonlinear dynamics of pursuit guidance for marine vehicles," *J. of Ship Research*, vol.37, no.4, pp.342-353, 1993.

[2] C. K. Angelopoulos, "String stability of multiple surface marine vessels," M.S. thesis, Mechanical and Aerospace Engineering Department, NPS, Monterey, California, 2011.

[3] D. Clarke, P. Gedling, and G. Hine, "The application of manuevering criteria in hull design using linear theory," *Transactions RINA*, vol. 124, 1982.

[4] C. A. Lyster, and H. L. Knights, "Prediction equations for ships' turning circles," *Transactions NECIES*, 1978-1979.

[5] M. Fugino, "Maneuverability in restricted waters: State of the art," The University of Michigan, Report No. 184, Aug., 1976.

[6] S. Inoue, M. Hirano, and K. Kijima, "Hydrodynamic derivatives on ship manuevering," *International Shipbuilding Progress*, vol. 28, no. 321, 1981.

[7] Z. Zaoijan, "Ship maneuvering and seakeeping," Lecture Notes, Shanghai Jiao Tong University, 2006.

[8] C. Daskam, "DDG-2025: Combating the FIAC threat," Project Report, NPS, Monterey California, 2012.

[9] F. A. Papoulias, "Dynamics of marine vehicles," Lecture Notes, NPS, Monterey California, 1993.

[10] F. A. Papoulias, "Cross track error and proportional turning rate guidance of marine vehicles," *J. of Ship Research*, vol.38, p.123, 1994.

[11] F. A. Papoulias, "Bifurcation analysis of line of sight vehicle guidance using sliding modes," *Int. J. of Bifurcation and Chaos*, vol. 1, p.4, 1991.

[12] F. A. Papoulias, "Stability considerations of guidance and control laws for autonomous underwater vehicles in the horizontal plane," in *Proceedings 7th International Symposium on Unmanned Underwater Submersible Technology*, Durham, New Hampshire, 1991.

[13] J.K. Hedrick, V. Garg, J.C. Gerdes, D.B. Maciuca, and D. Swaroop, "Longitudinal control development for IVHS fully automated and semi-automated system phase III," Final Report, University of California, Berkeley.

[14] J.K. Hedrick, M. Tomizuka, and P. Varaiya, “Control issues in automated highway systems,” *IEEE Control Systems Magazine*, 1994.

[15] D.V.A.H.G. Swaroop, “String stability of interconnected systems: An application to platooning in automated highway systems,” PhD Dissertation, University of California, Berkeley, April 1994.

INITIAL DISTRIBUTION LIST

1. Defense Technical Information Center
   Ft. Belvoir, Virginia

2. Dudley Knox Library
   Naval Postgraduate School
   Monterey, California